

Anisotropic Kondo effect in a valence-fluctuating system: CeNiIn

H. Fujii and T. Inoue

Faculty of Integrated Arts and Sciences, Hiroshima University, Hiroshima 730, Japan

Y. Andoh

Faculty of Education, Tottori University, Tottori 680, Japan

T. Takabatake

Faculty of Integrated Arts and Sciences, Hiroshima University, Hiroshima 730, Japan

K. Satoh, Y. Maeno, T. Fujita, J. Sakurai, and Y. Yamaguchi

Faculty of Science, Hiroshima University, Hiroshima 730, Japan

(Received 21 November 1988)

Measurements of magnetic susceptibility, electrical resistivity, thermoelectric power, and thermal expansion have been made on CeNiIn single crystals with a hexagonal Fe₂P-type structure. The results indicate that CeNiIn is a valence-fluctuating system with a significantly anisotropic Kondo effect which comes from anisotropic *c-f* mixing along the *a* and *c* axes. Specific-heat measurements on a CeNiIn polycrystal sample reveal that the magnetic contribution divided by temperature C_m/T takes a minimum around 20 K and reaches 60 mJ/K² mole around $T=2$ K, which is still ten times larger than that of LaNiIn with no 4*f* electron

I. INTRODUCTION

In the course of our research on new Kondo compounds, we have found that isostructural and isoelectronic ternary compounds Ce*T*In with *T*=Ni, Pd, and Pt display such interesting properties as Kondo lattice or valence-fluctuating states depending on the degree of mixing of *f* electrons with the conduction band near the Fermi surface.¹⁻⁴ Our results, obtained using polycrystal samples, can be summarized as follows.

CeNiIn is a valence-fluctuating system with Kondo-like behavior; the magnetic scattering resistivity ρ_m exhibits a broad peak around 100 K and a $\ln T$ dependence above 120 K. The inverse susceptibility χ^{-1} shows a weaker temperature variation than the Curie-Weiss behavior for free ions of Ce³⁺ above 30 K, and the thermoelectric power *S* takes a huge but broad peak of 50 μ V/K near 120 K, and an additional shoulder near 18 K.¹ CePdIn is an antiferromagnetic heavy-fermion system with $T_N=1.8$ K and specific heat versus temperature ratio $C_m/T=700$ mJ/mole K² at 70 mK.^{2,3} CePtIn is a nonmagnetic heavy-fermion system with $C_m/T=500$ mJ/mole K² (Ref. 2) below 1.0 K, and shows no sign of any phase transition at least down to 50 mK.⁴ All of these compounds crystallize in a hexagonal Fe₂P-type structure with space group $P\bar{6}2m$.⁵ In such a low symmetric crystal, we can expect a huge anisotropy in magnetic, transport, and thermal properties. So, it is very important to study physical properties using single crystals for the Ce*T*In systems.

In this paper, we present results of magnetic susceptibility, electrical resistivity, thermoelectric power, and thermal expansion measurements on the CeNiIn single

crystals. Specific heat has been also measured on CeNiIn and LaNiIn polycrystal samples, and the electronic specific-heat coefficient γ in CeNiIn was determined. In addition, magnetic measurements on a NdNiIn single crystal have been performed to obtain information on the crystalline electric field (CEF) effects in CeNiIn, since NdNiIn has stable 4*f* electrons and is suitable for determining the CEF parameters in this system.

Polycrystal samples were prepared by arc melting the constituent metals in a water-cooled copper hearth under a Ti-gettered flowing argon atmosphere. The ingots were turned over and remelted several times to ensure homogeneity. Single crystals were grown by a Czochralski method using a triarc furnace.⁶

II. RESULTS AND DISCUSSION

Temperature dependence of susceptibility measured along the *a* and *c* axes is shown in Fig. 1 for the CeNiIn single crystal. Both of the susceptibilities along the *a* and *c* axes χ_a and χ_c indicate not only a weaker temperature variation than the Curie-Weiss behavior for free ions of Ce³⁺, but also show anomalies around $T_M=120$ K, suggesting that CeNiIn is in a valence fluctuating state. The susceptibility χ_a is larger than χ_c in all of the measured temperature ranges. It is worth noting that this anisotropy cannot be accounted for by the CEF effects, which will be discussed later.

Electrical resistivity and thermoelectric power along the *a* and *c* axes are shown in Figs. 2(a) and (b) as a function of temperature. The magnitude of the *a*-axis resistivity ρ_a is three times larger than that of ρ_c , which was confirmed by repeating measurements of resistivity for two or three different kinds of single crystals. It is no-

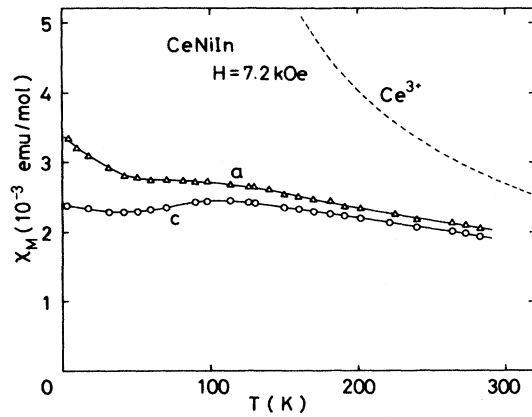


FIG. 1. Susceptibility along the a and c axes as a function of temperature for a CeNiIn single crystal. The dotted line represents the Curie susceptibility expected from the free Ce^{3+} ion with one $4f$ electron.

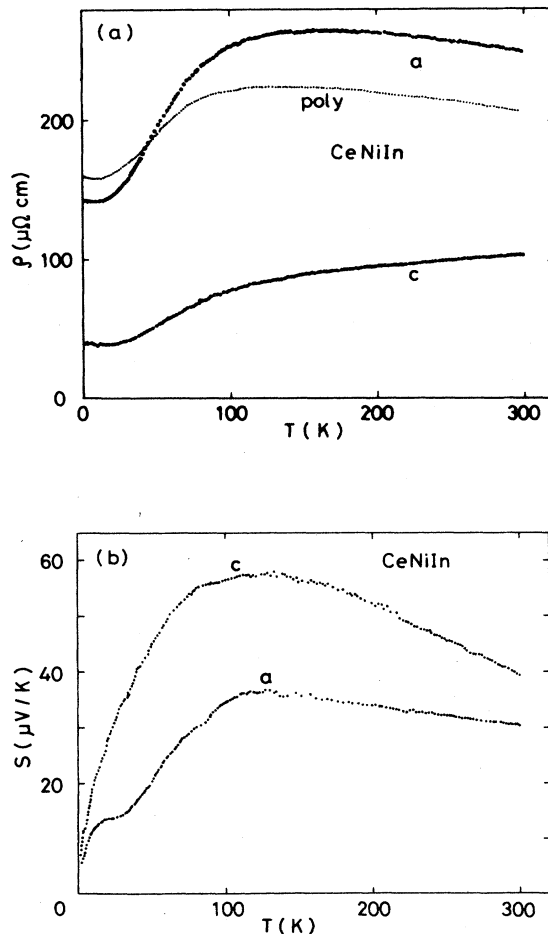


FIG. 2. (a) Electrical resistivity and (b) thermoelectric power along the a and c axes as a function of temperature for CeNiIn single crystals.

ticed that ρ_a exhibits a maximum around T_M and a $\ln T$ dependence in high-temperature ranges, whereas ρ_c decreases with decreasing temperature without anomaly. Such significantly different temperature dependences indicate that the Kondo scattering occurs mainly in the c plane. As is evident from Fig. 2(b), anisotropic behavior is observable in the a - and c -axis thermoelectric powers S_a and S_c . Both S_a and S_c are positive in all of the measured temperature regions and show maxima of $36 \mu V/K$ and $58 \mu V/K$, respectively, around T_M , where ρ_a takes a maximum. However, another shoulder appears around 40 K only in S_a . The presence of a shoulder in $S(T)$ has been observed in nonmagnetic dense Kondo compounds such as CeCu₆ (Ref. 7) and CePd₃ (Ref. 8).

In the thermal expansion along the a and c axes, anisotropic behavior is also observed as shown in Fig. 3, where $\Delta L = L(T) - L(300 K)$ is plotted as a function of temperature. The a axis shrinks remarkably with decreasing temperature, and its thermal expansion coefficient takes a maximum around T_M , while the c axis shrinks slightly with decreasing temperature down to 120 K, below which it starts to elongate. This behavior also suggests the significant anisotropy in c - f mixing in CeNiIn, since anomalous thermal expansion is thought to correlate strongly with valence-fluctuating states.

Magnetic measurements on a NdNiIn single crystal have been carried out to obtain information on the CEF effects in CeNiIn. The magnetization curve and inverse susceptibility measured along the a and c axes are shown in Figs. 4(a) and (b). NdNiIn is a simple ferromagnet with $T_c = 20$ K. The CEF effects appear in the magnetization curve at 4.2 K and paramagnetic susceptibility along the a and c axes. In fact, the saturation magnetic moment per Nd atom μ_{Nd} deduced from M versus H curves at 4.2 K is much smaller than that expected for the Nd^{3+} free ion, $3.2\mu_B$, although the effective number of Bohr magnetons estimated from the Curie-Weiss law is in good agreement with the Nd^{3+} free ion value $3.62\mu_B$. The paramagnetic Curie temperatures along the a and c axes are $\Theta = 4.0$ K and $\Theta_c = 9.0$ K, respectively. Below 60 K, both χ_a^{-1} and χ_c^{-1} deviate from the Curie-Weiss law, suggesting the importance of higher-order CEF effects.

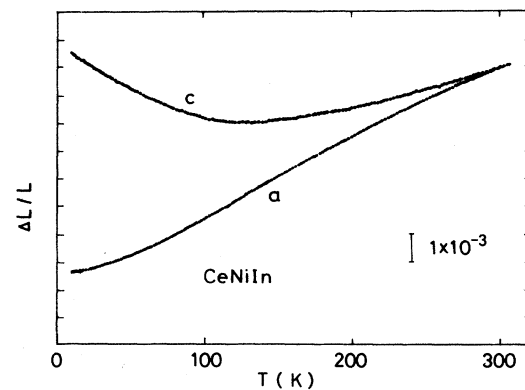


FIG. 3. Temperature dependence of thermal expansion along the a and c axes for CeNiIn single crystals.

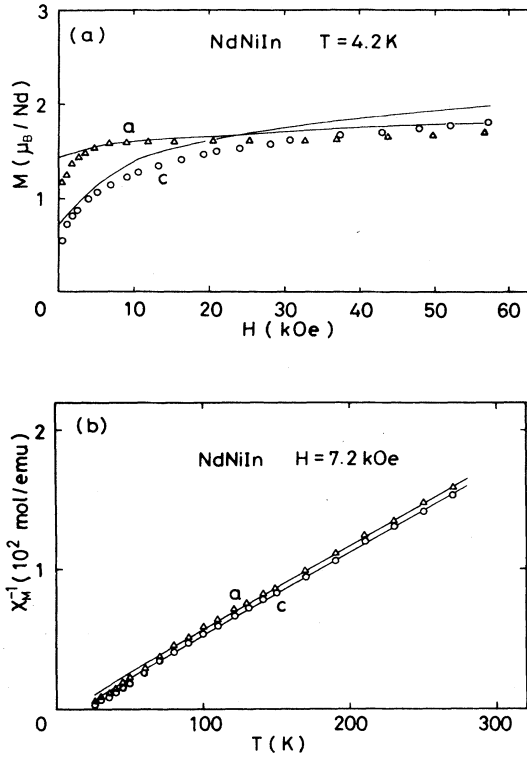


FIG. 4. (a) Magnetization and (b) inverse susceptibility along the *a* and *c* axes as functions of magnetic field and temperature, respectively, for a NdNiIn single crystal. The full lines represent magnetization curves and temperature variations of inverse susceptibilities calculated using $B_2^0 = -0.17$ K, $B_4^0 = 2.6 \times 10^{-2}$ K, $B_6^0 = -6.8 \times 10^{-5}$ K, $B_6^6 = -3.4 \times 10^{-3}$ K, and $\lambda = 7.8$ mole/emu.

In order to determine the CEF parameters for NdNiIn, we introduce the effective single-ion Hamiltonian, including the CEF, molecular field, and applied magnetic field as follows:

$$\chi_{\text{CEF}}^i = \frac{g^2 \mu_B^2}{kT} \left[\sum_{\substack{n,m \\ E_m = E_n}} \frac{|\langle m | J_i | n \rangle|^2}{Z} \exp(-E_n/kT) - \left(\sum_n \langle n | J_i | n \rangle \exp(-E_n/kT) / Z \right)^2 \right] + 2g^2 \mu_B^2 \left[\sum_{\substack{m,n \\ E_m \neq E_n}} \langle m | J_i | n \rangle^2 (E_m - E_n)^{-1} \exp(-E_n/kT) / Z \right]. \quad (4)$$

In the mean-field approximation, the effective susceptibility χ_i is expressed as

$$\chi^i = \chi_{\text{CEF}}^i / (1 - \lambda \chi_{\text{CEF}}^i). \quad (5)$$

We determined the CEF parameters from a least-square fitting of the data of M and χ^{-1} along the *a* and *c* axes for NdNiIn.⁹ The best fit is obtained with the following pa-

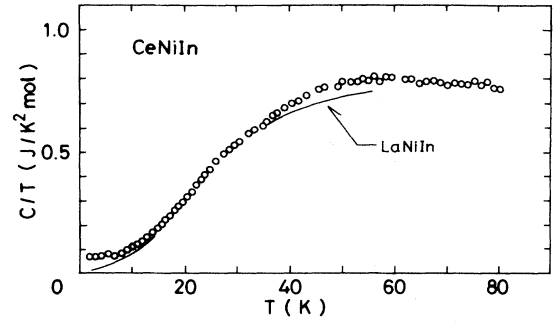


FIG. 5. Temperature dependence of C/T for CeNiIn in the temperature range between 1.8 and 80 K. The data for LaNiIn are also shown by a solid line, for comparison.

$$H = H_c - g\mu_B J_z (H + H_m). \quad (1)$$

Here, H_c is the CEF Hamiltonian, H the applied magnetic field, and H_m the molecular field. In a hexagonal lattice, H_c is represented by

$$H_c = B_2^0 O_2^0 + B_4^0 O_4^0 + B_6^0 O_6^0 + B_6^6 O_6^6, \quad (2)$$

where B_n^m is the CEF parameter and O_n^m is the Steven's operator. The molecular field H_m can be written $H_m = \lambda M$, where λ is the molecular-field coefficient and M the thermal average of magnetization which is given as follows:

$$M = \sum_n g\mu_B J_n \exp(-E_n/kT) / Z. \quad (3)$$

Here, Z is the partition function expressed by $Z = \sum_n \exp(-E_n/kT)$, $J_n = \langle n | J_z | n \rangle$, and E_n is the eigenvalue of the n th crystalline-field eigenfunction $|n\rangle$.

The CEF susceptibility χ_{CEF}^i without exchange interaction along the *i* direction is given by

rameters: $B_2^0 = -0.17$ K, $B_4^0 = 2.6 \times 10^{-2}$ K, $B_6^0 = -6.8 \times 10^{-5}$ K, $B_6^6 = -3.4 \times 10^{-3}$ K, and $\lambda = 7.8$ mole/emu. The calculated curves of M and χ^{-1} using these parameters are drawn by solid lines in Figs. 4(a) and (b). The fairly good fitting for both sets of the data suggest that anisotropies in M and χ^{-1} for NdNiIn can be qualitatively understood by the CEF effects. If we assume that Ce in CeNiIn is a well-defined Ce^{3+} state and the CEF in

CeNiIn is the same as in NdNiIn, then we can deduce the CEF parameters for CeNiIn according to a scaling law as $B_2^0 = -1.81$ K, and $B_4^0 = -0.82$ K. These parameters lead to $\chi_c > \chi_a$ in all measured temperature ranges, which is in contradiction to the experimental result, $\chi_c < \chi_a$. So it is clear that the anisotropy observed in χ along the a and c axes for CeNiIn originates in the anisotropic c - f mixing interactions rather than the CEF effects.

The ratio of specific heat to temperature C/T for CeNiIn is shown in Fig. 6 as a function of temperature, together with the data for nonmagnetic and isostructural LaNiIn, which are drawn by a solid line. The specific heat of LaNiIn below 11 K is well fitted with the sum of the electronic contribution γT with $\gamma = 9.1 \pm 0.2$ mJ/K² mole and the phonon contribution βT^3 with $\beta = 0.64 \pm 0.05$ mJ/K⁴ mole, from which the Debye temperature of $\Theta_D = 209 \pm 4$ K is obtained. The magnetic contribution C_m is estimated by subtracting the specific heat of the reference compound LaNiIn from that of CeNiIn. As shown in Fig. 6, C_m/T takes a minimum around 20 K, suggesting a spin-fluctuation contribution at low temperatures, and reaches 60 mJ/K² mole around $T = 2$ K. This value is one order of magnitude smaller than the other isostructural and isoelectronic compounds, CePdIn³ (Ref. 3) and CePtIn⁴ (Ref. 4), but it is still one order larger than LaNiIn with no $4f$ electron.

In summary, all the results obtained on the single crystals indicate that CeNiIn is a valence-fluctuating system with significantly anisotropic Kondo anomalies on magnetic, transport, and thermal properties. The anisotropic Kondo effect is thought to be due to anisotropic c - f mixing interactions along the a and c axes of the hexagonal Fe₂P-type structure. It is likely that the c - f mixing is

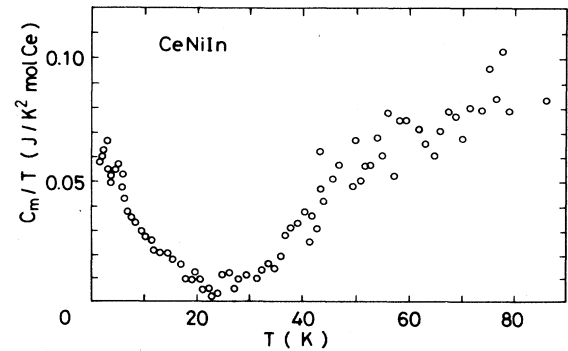


FIG. 6. Temperature dependence of C_m/T for CeNiIn, approaching $C_m/T = 60$ mJ/K² mole around 2 K.

strong for the Fermi surface perpendicular to the c axis, while a substantial part of Fermi surface parallel to the c axis has a weaker c - f mixing. To understand the anisotropic Kondo anomalies in CeNiIn, it is necessary to obtain detailed information¹⁰ on the electronic structure near the Fermi surface.

ACKNOWLEDGMENTS

The authors would like to thank Mr. Y. Iguchi for his assistance. This work was supported by a Grant-in-Aid for Scientific Research from the Ministry of Education, Science, and Culture of Japan.

¹H. Fujii, Y. Uwatoko, M. Akayama, K. Satoh, Y. Maeno, T. Fujita, J. Sakurai, H. Kamimura, and T. Okamoto, *Jpn. J. Appl. Phys. Suppl.* **26-3**, 549 (1987).

²Y. Maeno, M. Takahashi, T. Fujita, Y. Uwatoko, H. Fujii, and T. Okamoto, *Jpn. J. Appl. Phys. Suppl.* **26-3**, 545 (1987).

³K. Satoh, T. Fujita, Y. Maeno, Y. Uwatoko, and H. Fujii, in *Proceedings of the International Conference on Magnetism*, Paris, 1988 [*J. Phys. (Paris)* (to be published)].

⁴T. Fujita, K. Satoh, Y. Maeno, Y. Uwatoko, and H. Fujii, *J. Magn. Magn. Mater.* **76&77**, 133 (1988).

⁵R. Ferro, R. Marazza, and G. Romboldi, *Z. Metallkd.* **65**, 40 (1974).

⁶H. Sadamura, H. Fujii, and T. Okamoto, *IEEE Trans. J. Magn. Jpn.* **TJMJ-1**, 810 (1985).

⁷Y. Onuki and T. Komatsubara, *J. Magn. Magn. Mater.* **63&64**, 281 (1987).

⁸D. Jaccard, M. J. Besnus, and J. P. Kappler, *J. Magn. Magn. Mater.* **63&64**, 572 (1987).

⁹Y. Andoh, *J. Phys. Soc. Jpn.* **56**, 4075 (1987).

¹⁰See, for example, B. R. Cooper *et al.*, in *Handbook on the Physics and Chemistry of the Actinides*, edited by A. J. Freeman and G. H. Lander (Elsevier, New York, 1985), Vol. 2, p. 435.